Cell
PRESS

Open
ACCESS

Pain without Nociceptors?
Nav1.7-Independent Pain Mechanisms

Michael S. Minett,[1] Sarah Falk,[2] Sonia Santana-Varela,[1] Yury D. Bogdanov,[1] Mohammed A. Nassar,[1]
Anne-Marie Heegaard,[2] and John N. Wood[1,*]
[1]Molecular Nociception Group, Wolfson Institute for Biomedical Research, University College London, Gower Street, London WC1E 6BT, UK
[2]Department of Drug Design and Pharmacology, Faculty of Health and Medical Sciences, University of Copenhagen, Universitetsparken 2,
2100 Copenhagen, Denmark
*Correspondence: j.wood@ucl.ac.uk
http://dx.doi.org/10.1016/j.celrep.2013.12.033

SUMMARY

Nav1.7, a peripheral neuron voltage-gated sodium channel, is essential for pain and olfaction in mice and humans. We examined the role of Nav1.7 as well as Nav1.3, Nav1.8, and Nav1.9 in different mouse models of chronic pain. Constriction-injury-dependent neuropathic pain is abolished when Nav1.7 is deleted in sensory neurons, unlike nerve-transection-related pain, which requires the deletion of Nav1.7 in sensory and sympathetic neurons for pain relief. Sympathetic sprouting that develops in parallel with nerve-transection pain depends on the presence of Nav1.7 in sympathetic neurons. Mechanical and cold allodynia required distinct sets of neurons and different repertoires of sodium channels depending on the nerve injury model. Surprisingly, pain induced by the chemotherapeutic agent oxaliplatin and cancer-induced bone pain do not require the presence of Nav1.7 sodium channels or Nav1.8-positive nociceptors. Thus, similar pain phenotypes arise through distinct cellular and molecular mechanisms. Therefore, rational analgesic drug therapy requires patient stratification in terms of mechanisms and not just phenotype.

INTRODUCTION

Pain afflicts a fifth of the population; there is an urgent need for new analgesic drugs with minimal side effects. There is strong evidence that, in most chronic pain conditions arising from nerve damage or inflammation, peripheral nerve block can cause pain relief in humans, proving that peripheral drive is critical to chronic pain (Aguirre et al., 2012). However, our understanding of the functional diversity of peripheral sensory neurons is limited, although attempts have been made to link histochemical markers to function with limited success. The developmental complexity of sensory neuron specification has been extensively

analyzed (Lallemend and Ernfors, 2012), but the links to function remain obscure. Here, we explore the role of voltage-gated sodium channels in different pain syndromes and provide evidence for a diversity of mechanisms in peripheral pain pathways that may help to explain recent failures to develop new analgesic drugs targeting peripheral neurons.

Studies of human monogenic disorders of pain perception have drawn attention to the voltage-gated sodium channels in sensory neurons (Eijkelkamp et al., 2012; Waxman, 2013), particularly Nav1.7 as a potential drug target, because loss of function in this channel leads to chronic insensitivity to pain (CIP) (Cox et al., 2006, Goldberg et al., 2007). Modeling this loss-of-function syndrome in mice recapitulates the human pain-free phenotype; acute thermal and mechanical insults have no behavioral consequences, whereas inflammatory pain is also abolished in inbred mouse strains lacking Nav1.7 in peripheral neurons (Minett et al., 2012; Nassar et al., 2004). Although the analgesia associated with loss of Nav1.7 function is dramatic, modality-specific pain therapies are more desirable for most chronic pain conditions where general analgesia could lead to inadvertent self-harm.

Earlier studies suggested that seemingly similar neuropathic pain models differed mechanistically (Kim et al., 1997). Neuropathic pain can be either sympathetically maintained or sympathetically independent (Roberts, 1986). Here, we examined a number of models including the spinal nerve transection (SNT) model (Kim and Chung, 1992) and the chronic constriction injury (CCI) model (Bennett and Xie, 1988). In the SNT model, mechanical and cold allodynia are associated with the invasion of the dorsal root ganglion (DRG) by postganglionic adrenergic sympathetic axons (Ramer and Bisby, 1998a, 1998c). In contrast, CCI is thought to trigger an immune response leading to a "neuritis" (Campbell and Meyer, 2006), where surgical lumbar sympathectomy produces no signification change in mechanical or cold allodynia (Kim et al., 1997). A further model associated with nerve damage, the oxaliplatin model of chemotherapeutic-induced neuropathic pain, was investigated (Renn et al., 2011) because painful neuropathies affect a third of all patients who undergo chemotherapy (Velasco and Bruna, 2010). Additionally, we examined spontaneous and movement-evoked pain behavior associated with cancer-induced bone pain in a syngeneic model
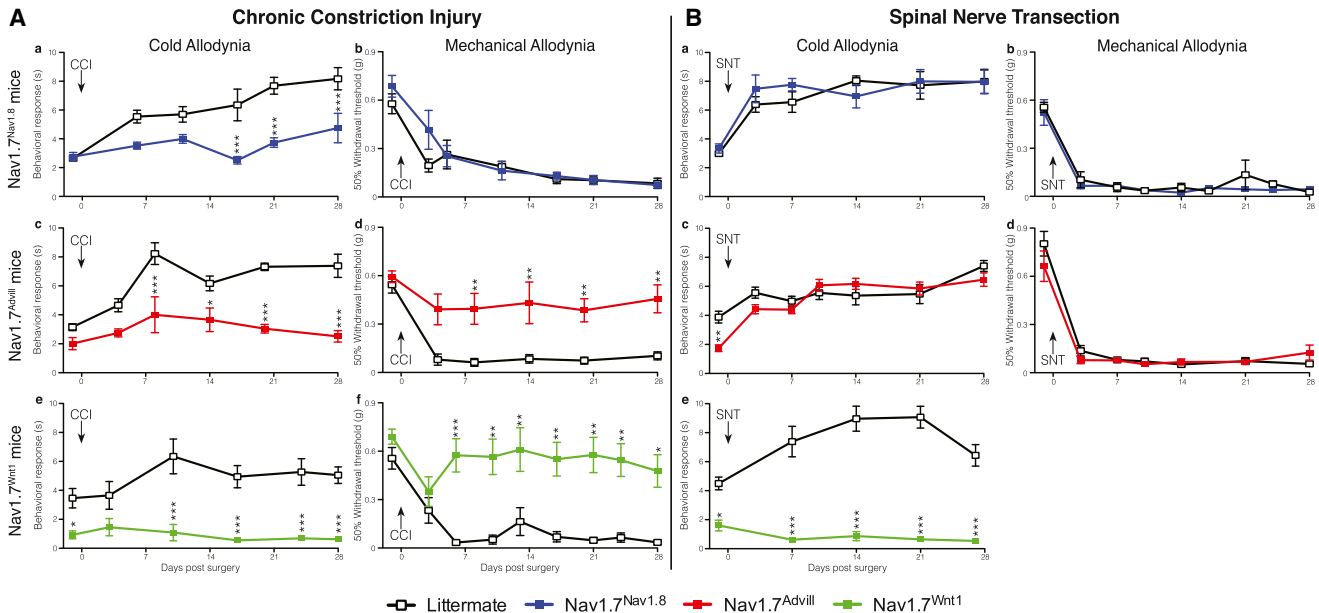
CrossMark

Figure 1. Comparison of Transgenic Mice Reveals Tissue-Specific Roles for Nav1.7 in Mechanical and Cold Allodynia after CCI Surgery as Well as a Role Specifically in Sympathetic Neurons after SNT Surgery

Behavioral responses of different Nav1.7 tissue-specific knockouts to the von Frey and acetone test following CCI (A) and L5 SNT surgery (B). Nav1.7[Nav1.8] (blue squares, n = 9) do not develop CCI-induced cold allodynia (Aa) but do develop mechanical allodynia (Ab) in comparison to littermate mice (white squares, n = 8). Nav1.7[Advill] (red squares, n = 8) do not develop CCI-induced cold (Ac) or mechanical allodynia (Ad) in comparison to littermate mice (white squares, n = 9). Nav1.7[Wnt1] (green squares, n = 9) do not develop CCI-induced cold (Ae) nor mechanical allodynia (Af) in comparison to littermate mice (white squares, n = 6). Nav1.7[Nav1.8] (blue squares, n = 6) develop both SNT-induced cold (Ba) and mechanical allodynia (Bb) in comparison to littermate mice (white squares, n = 6). Nav1.7[Advill] (red squares, n = 6) develop both SNT-induced cold (Bc) and mechanical allodynia (Bd) in comparison to littermate mice (white squares, n = 9). Nav1.7[Wnt1] (green squares, n = 9) do not develop SNT-induced cold allodynia (Be) in comparison to littermate mice (white squares, n = 12). Data analyzed by two-way analysis of variance followed by the Bonferroni post hoc test. Results are presented as mean ± SEM. **$p < 0.01$ and ***$p < 0.001$ (individual points). See also Figure S1.

of metastatic bone cancer. Bone metastasis is a common complication for patients suffering from advanced lung, breast, prostate, or skin cancers and is the most common source of severe cancer pain (Kinnane, 2007; Mercadante, 1997).

Here, we have used models of neuropathic and cancer-induced bone pain to investigate the role of Nav1.7, as well as other voltage-gated sodium channels in the development of pain syndromes. We crossed floxed (*Scn9a*) Nav1.7 mice with different tissue-restricted Cre mouse strains to generate nociceptor-specific (Nav1.7[Nav1.8]), pan-DRG (Nav1.7[Advill]), and pan-DRG and sympathetic (Nav1.7[Wnt1]) Nav1.7 knockout mouse strains and examined the effects on pain behavior. We also compared the effects of deleting Nav1.7 in utero or in adult animals to examine any developmental effects that may contribute to CIP. Surprisingly, we found that classical nociceptors defined by the presence of the sodium channel Nav1.8, or the sodium channel Nav1.7 that have been linked to all forms of acute and inflammatory pain (Minett et al., 2012; Nassar et al., 2004) are not required for ongoing pain in models of cancer-induced bone pain or oxaliplatin-induced neuropathic pain. We also found that phenotypically identical pain syndromes are induced through different molecular mechanisms in distinct sets of sensory and sympathetic neurons. This functional redundancy raises questions about the organization of peripheral pain pathways and strategies for treating pain.

RESULTS

Generation of Nav1.7 Conditional Knockout Mouse Strains

We used the Cre-loxP system to generate a number of conditional Nav1.7 knockout mouse strains. Floxed (*Scn9a*) Nav1.7 mice were crossed with strains where Cre expression is driven by either the Nav1.8 promoter (Nav1.7[Nav1.8]), expressed in >90% of neurons expressing markers of nociceptors (Nassar et al., 2004; Shields et al., 2012), the Advillin promoter (Nav1.7[Advill]), expressed in all DRG neurons (Minett et al., 2012), and the Wnt1 promoter (Nav1.7[Wnt1]), expressed in tissue derived from the neural tube, including sensory and sympathetic neurons (Danielian et al., 1998).

Pain-Modality-Specific Neurons and Nav1.7 in Neuropathic Pain Models

The three different tissue-specific Nav1.7 transgenic knockout mouse strains were examined after CCI of the sciatic nerve, or SNT of the fifth lumbar segment. Both surgical models produce robust cold and mechanical allodynia. In DRG neurons, Nav1.7 mediates the increased sensitivity to both the acetone and the von Frey test following CCI surgery (Figure 1A). A comparison of the Nav1.7[Nav1.8] and Nav1.7[Advill] behavioral responses reveals a modality-specific role for Nav1.7 within different DRG

subpopulations. Nav1.7[Nav1.8] mice do not develop acetone-induced cold allodynia (Figure 1Aa) but show normal mechanical allodynia (Figure 1Ab). This is also true for the partial nerve ligation (Seltzer et al., 1990) surgically induced neuropathic pain model (Figures S1A and S1B). In contrast, deleting Nav1.7 from all DRG neurons attenuates both cold and mechanical allodynia (Figures 1Ac–1Af). Figure 1B demonstrates that Nav1.7 expression within DRG neurons is not critical for cold or mechanical allodynia in the sympathetically mediated SNT model. Both Nav1.7[Nav1.8] and Nav1.7[Advill] mice develop both cold and mechanical allodynia normally following SNT surgery (Figures 1Ba–1Bd), demonstrating that pain associated with the SNT model does not directly arise from Nav1.7-positive nociceptors, unlike the CCI model. In contrast, Nav1.7[Wnt1] mice develop neither cold (Figure 1Be) nor mechanical allodynia (Minett et al., 2012) demonstrating that Nav1.7 expressed within peripheral sympathetic neurons is essential for the SNT-induced mechanical and cold allodynia.

Interactions between sympathetic neurons and the neuronal somata of DRG neurons have been described since the era of Ramón y Cajal in the 19th century (García-Poblete et al., 2003). Nerve injury has been shown to induce increased sympathetic sprouting into the DRG (McLachlan et al., 1993; Ramer and Bisby, 1998c). A high innervation density of sympathetic axons (highlighted by yellow arrow heads) was found within ipsilateral L4 DRG 30 days following SNT surgery (Figure 2A), in comparison to contralateral L4 DRG (Figure 2B). These sprouting sympathetic axons form "baskets" around the DRG cell body of large myelinated DRG neurons (McLachlan et al., 1993; Ramer and Bisby, 1998a), an example of which can be seen in Figure 2C. Quantification of sympathetic sprouting following SNT surgery shows that Nav1.7[Nav1.8] and Nav1.7[Advill] mice are indistinguishable from littermate controls (Figure 2D). In contrast, Nav1.7[Wnt1] mice show the same low level sympathetic sprouting density in the ipsilateral as the contralateral L4 DRG following SNT surgery. No significant change in DRG size was observed in the three Nav1.7 knockout mouse strains or littermate controls. Nav1.7 expression within sympathetic neurons is therefore required for sympathetic sprouting following nerve injury. Inhibition of Nav1.7-mediated sympathetic sprouting is associated with a loss of cold (Figure 1Be) and mechanical allodynia in Nav1.7[Wnt1] mice (Minett et al., 2012).

Global deletion of other voltage-gated sodium channels, such as Nav1.3, Nav1.8, or Nav1.9 does not reduce the sympathetic sprouting density following nerve damage (Figure 2E). Performing a chemical sympathectomy on Nav1.7[Advill] mice prior to SNT surgery (Figure 2F) recapitulates the Nav1.7[Wnt1] behavioral phenotype (Minett et al., 2012). It has previously been reported that approximately 10% of lumbar DRG neurons are tyrosine hydroxylase (TH) positive, although they are thought to be dopaminergic because they lack the enzymes required for norepinephrine or epinephrine production (Brumovsky et al., 2006). Microarray analysis of DRG from mice where the Nav1.8-positive DRG population has been ablated (Nav1.8[DTA]) shows a significant decrease in TH (10-fold) in comparison to littermates, indicating an overlap between the Nav1.8 and TH-positive neurons (Abrahamsen et al., 2008). However, the disruption of the Nav1.8-positive DRG population in the

Nav1.7[Nav1.8] mice does not alter the development of pain following SNT. Together this suggests that TH-positive DRG subpopulation is not critical for the development SNT-induced cold and mechanical allodynia.

The combination of chemical sympathectomy and the loss of Nav1.7 from all DRG neurons shows greater attenuation of SNT-induced mechanical allodynia than chemical sympathectomy alone (Figure 2F), suggesting the nociceptors contribute to SNT-evoked mechanical allodynia. Cutaneous injection of the sympathetic transmitter norepinephrine rekindles the spontaneous pain and dynamic mechanical hyperalgesia in posttraumatic neuralgia patients, which had been relieved by sympathetic block (Torebjörk et al., 1995). Peripheral sensory neurons have been shown to develop noradrenergic sensitivity following nerve lesion through an upregulation of α2-adrenoceptors in intact afferent fibers (Baron et al., 1999). Interestingly, intraplantar injection of norepinephrine induces mechanical allodynia in Nav1.7[Wnt1] mice 14 days after SNT surgery (Figure 2G). This means that peripheral pain pathways can be activated in the absence of Nav1.7 after nerve damage. Norepinephrine-induced SNT mechanical allodynia can be detected within 10 min and is still apparent 5 days postinjection. Importantly, intraplantar injection of norepinephrine does not induce mechanical allodynia in naive mice (Figure S2). Norepinephrine-mediated coupling between sympathetic and DRG neurons is thus critical for the development of pain in the sympathetically mediated SNT neuropathic pain model. Sympathetic sprouting following SNT is mainly associated with large diameter sensory neurons (Xie et al., 2011), as is the vast majority of norepinephrine-evoked spontaneous neuronal activity following SNT (Liu et al., 1999).

Distinct Modality-Specific Roles for Nav1.3, Nav1.8, and Nav1.9 in Neuropathic Pain

A comparison of the behavioral responses of Nav1.3, Nav1.8, and Nav1.9 global knockout mouse strains in the CCI (Figure 3A) and SNT (Figure 3B) neuropathic pain models reveals modality-specific roles for these sodium channels. Deletion of Nav1.3 reduces cold allodynia (Figure 3Aa) as well as the magnitude of mechanical allodynia (Figure 3Ab) following CCI surgery. However, mice lacking Nav1.8 show an attenuated response to acetone-induced cold allodynia (Figure 3Ac) but develop mechanical allodynia normally (Figure 3Ad). The same is also true for Nav1.9 knockout mice (Figures 3Ae and 3Af). Interestingly, Figure 3B shows that all these behavioral phenotypes are restricted to the CCI models of neuropathic pain. Both cold and mechanical allodynia develop normally in mice lacking Nav1.3 (Figures 3Ba and 3Bb), Nav1.8 (Figures 3Bc and 3Bd), and Nav1.9 (Figures 3Be and 3Bf) following SNT surgery. Additionally, sympathetic sprouting into the DRG develops normally in the Nav1.3, 1.8, and 1.9 global knockout mouse strains (Figure 2E), demonstrating that only Nav1.7 is required for sympathetic sprouting following SNT surgery.

Oxaliplatin-Induced Pain and Cancer-Induced Bone Pain Are Nav1.7 Independent

Both Nav1.7[Advill] (Figures S3A and S3B) and Nav1.7[Wnt1] (Figures 4A and 4B) mice develop mechanical and cold allodynia normally
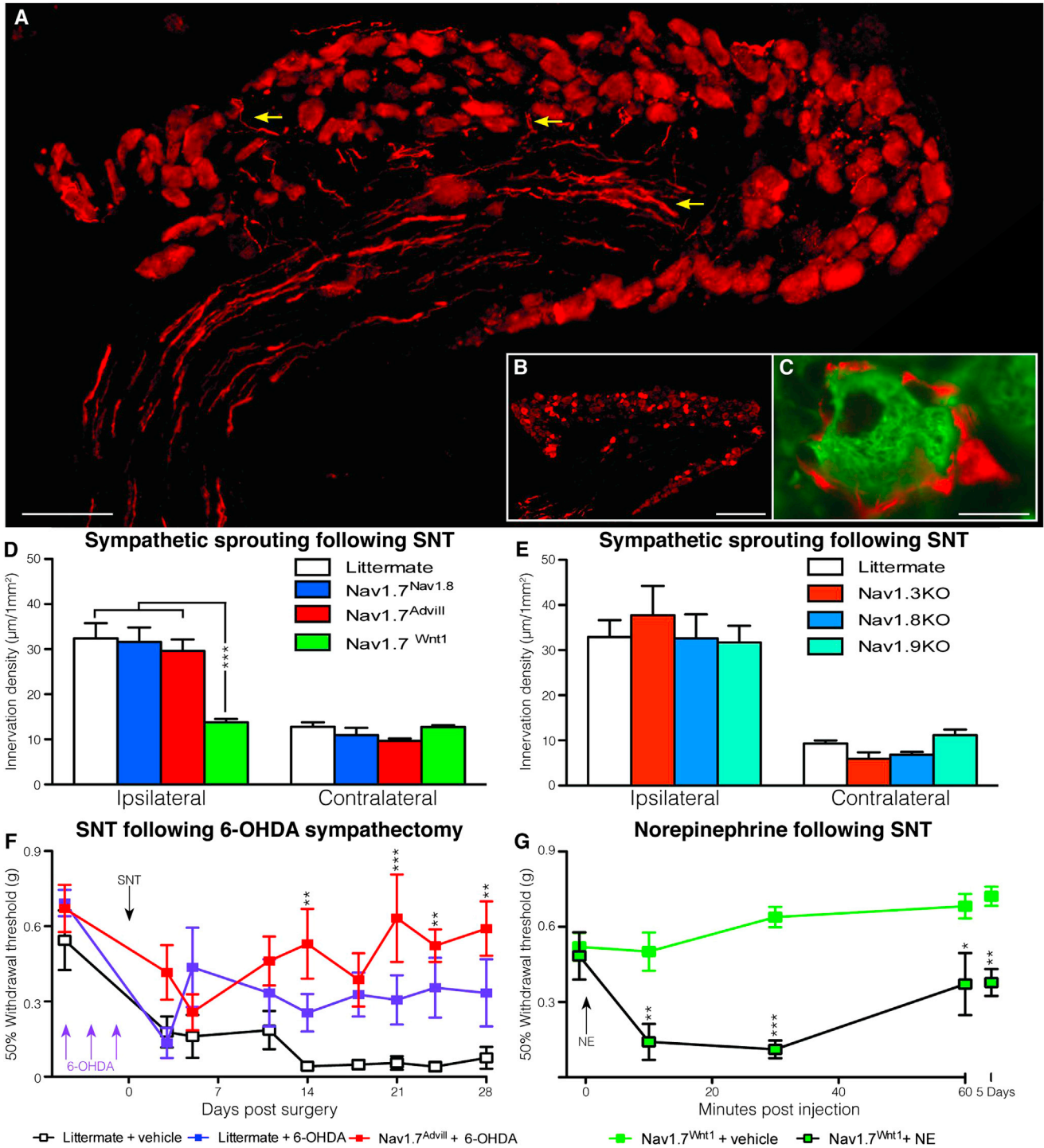
Figure 2. Spinal Nerve Transection Fails to Trigger Sympathetic Sprouting in Nav1.7[Wnt1] Mice, which Can Be Sensitized by Norepinephrine

(A) Yellow arrows show examples of sympathetic sprouting (tyrosine hydroxylase, red) into the ipsilateral DRG following SNT surgery (scale bar = 100 μm).

(B) An example of a contralateral DRG showing no sympathetic sprouting (tyrosine hydroxylase, red) following SNT surgery (scale bar = 200 μm).

(C) An example of a sympathetic "basket" (tyrosine hydroxylase, red) formed around a large diameter (N52, green) DRG neuron (scale bar = 20 μm).

(D) Quantitation of sympathetic sprouting into the ipsilateral and contralateral L4 DRG following SNT. Littermates (white columns, n = 3), Nav1.7[Nav1.8] (blue columns, n = 3), Nav1.7[AdvIll] (red columns, n = 3), and Nav1.7[Wnt1] (green columns, n = 3).

(E) Quantitation of sympathetic sprouting into the L4 DRG following SNT. Littermates (white columns, n = 3), Nav1.3KO (orange columns, n = 3), Nav1.8KO (light blue columns, n = 3), and Nav1.9KO (turquoise columns, n = 3).
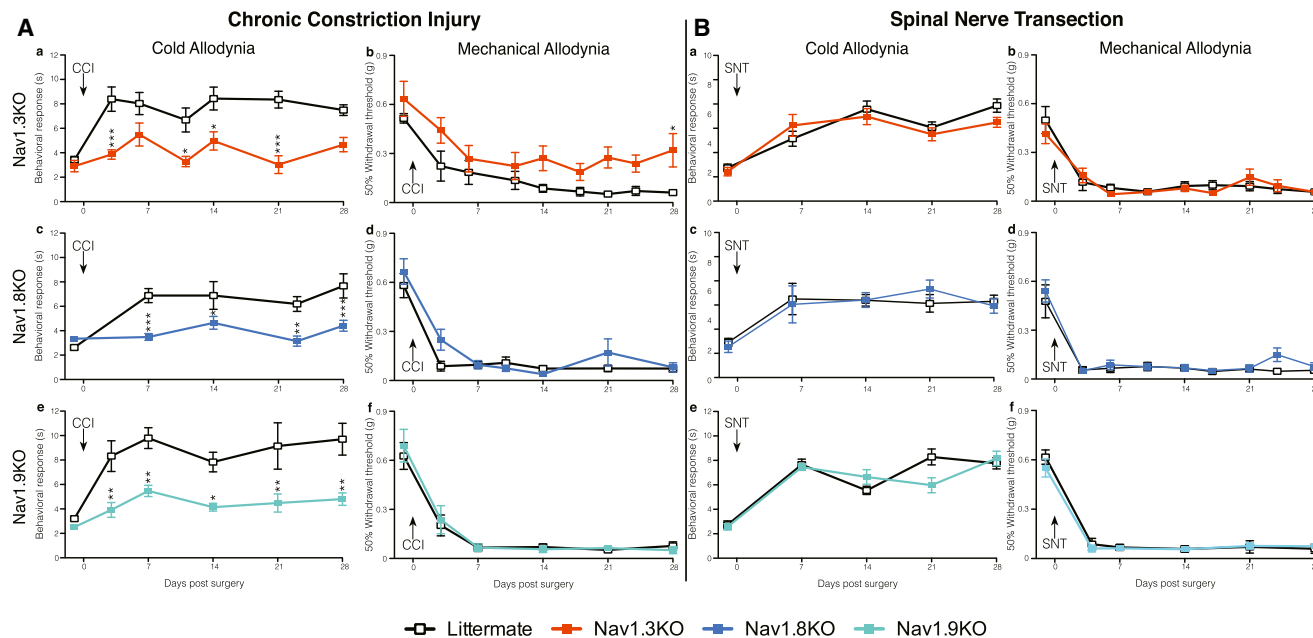
(legend continued on next page)

Figure 3. Behavioral Responses of Nav1.3, Nav1.8, and Nav1.9 Knockout Mice Reveal Critical Roles in Modality-Specific Responses to CCI-Induced Pain but Not Sympathetically Mediated SNT Pain

Behavioral von Frey and acetone responses of Nav1.3, Nav1.8, or Nav1.9 knockouts following CCI (A) and L5 SNT surgery (B). Nav1.3KO mice (orange squares, n = 6) show reduced CCI-induced cold allodynia (Aa) and mechanical allodynia (Ab) in comparison to littermate mice (white squares, n = 10). Nav1.8KO mice (light blue squares, n = 8) show diminished CCI-induced cold allodynia (Ac) but do develop mechanical allodynia (Ad) in comparison to littermate mice (white squares, n = 10). Nav1.9KO mice (turquoise squares, n = 8) show diminished CCI-induced cold allodynia (Ae) but do develop mechanical allodynia (Af) in comparison to littermate mice (white lines, n = 8). Nav1.3KO mice (orange squares, n = 10) develop both L5 SNT-induced cold (Ba) and mechanical allodynia (Bb) in comparison to littermate mice (white squares, n = 8). Nav1.8KO mice (light blue squares, n = 8) develop L5 SNT-induced cold (Bc) and mechanical allodynia (Bd) in comparison to littermate mice (white squares, n = 8). Nav1.9KO mice (turquoise squares, n = 10) develop L5 SNT-induced cold (Be) and mechanical allodynia (Bf) in comparison to littermate mice (white squares, n = 7). Data analyzed by two-way analysis of variance followed by the Bonferroni post hoc test. Results are presented as mean ± SEM. **p < 0.01 and ***p < 0.001 (individual points).

following oxaliplatin treatment when compared to littermate controls. This shows that the expression of Nav1.7, within either DRG or sympathetic neurons is not required for this pain syndrome. Similarly, global deletion of Nav1.3, Nav1.8, or Nav1.9 does not attenuate either mechanical or cold allodynia in this model (Figures S3C–S3H) despite the suggestion that enhanced Nav1.8 expression could contribute to oxaliplatin-induced cold pain (Descoeur et al., 2011). Finally, both mechanical and cold allodynia develop normally in Nav1.8DTA mice (Figures 4C and 4D). The oxaliplatin model thus has a distinct underlying mechanism from both sympathetically dependent and independent surgically induced neuropathic pain models, as well as inflammatory pain (Minett et al., 2012; Nassar et al., 2004) and does not require the presence of Nav1.8-positive nociceptors.
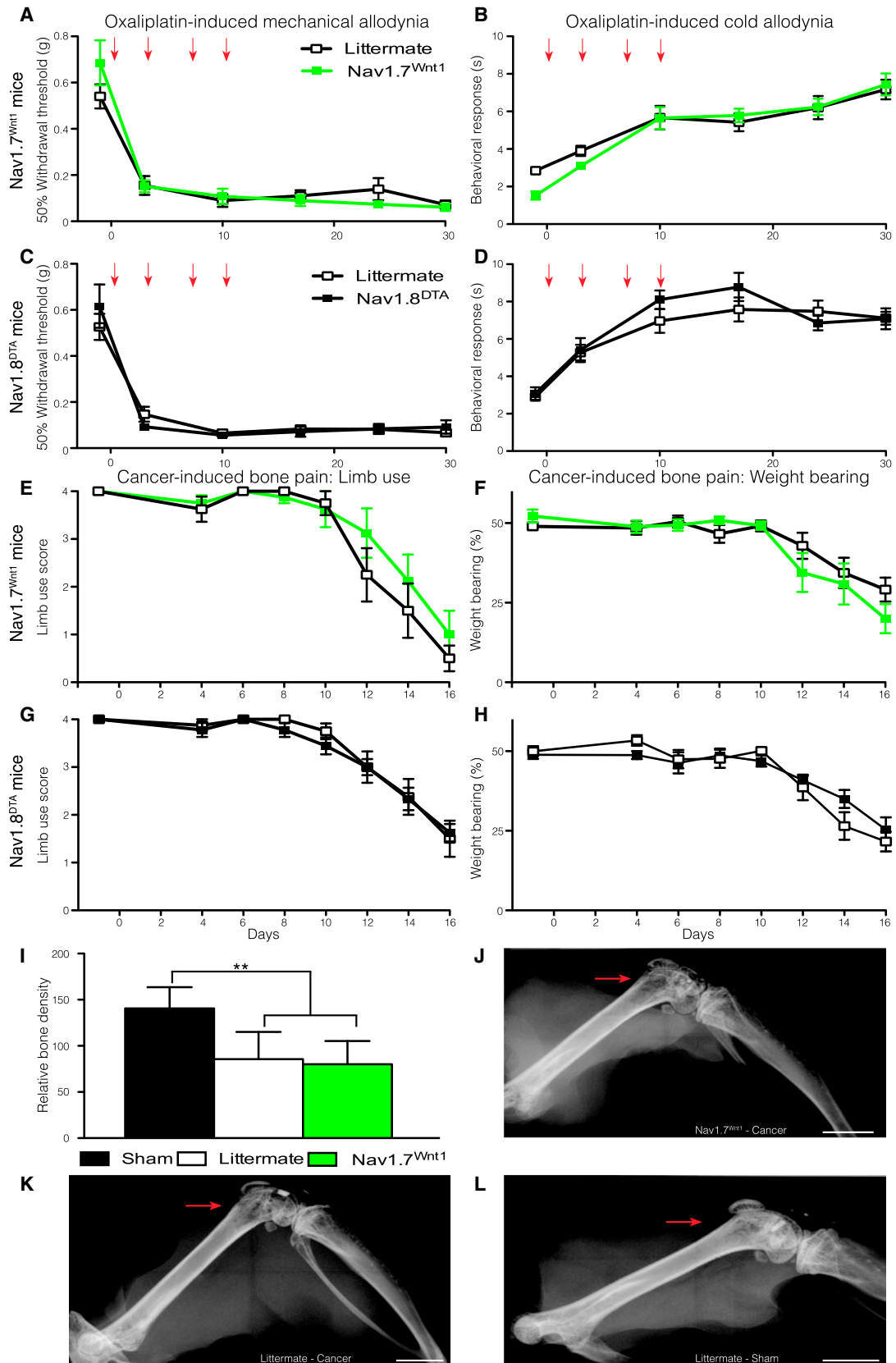
In a mouse model of metastatic cancer pain induced by intrafemoral injection of syngeneic LL/2 lung carcinoma cells, we found that, as with oxaliplatin-evoked pain, deleting Nav1.7 expression in the peripheral nervous system did not result in the loss of pain behavior. No behavioral deficits were observed in either limb use or weight-bearing ratio (Figures 4E and 4F), although deleting Nav1.7 from the peripheral nervous system produces striking behavioral deficits in all acute, inflammatory, and surgically induced neuropathic pain models tested (Minett et al., 2012; Nassar et al., 2004). Ablation of Nav1.8-positive neurons in the Nav1.8DTA mouse strain leads to the loss of many pain modalities (Abrahamsen et al., 2008) but surprisingly does not diminish the development of cancer-induced bone pain (Figures 4G and 4H). No significant differences in the level of bone degradation were observed (Figure 4I). Example X-rays from a Nav1.7Wnt1 mouse (Figure 4J) and a littermate mouse (Figure 4K) both show pronounced bone degradation (highlighted by the red arrows) in comparison to sham-operated mice (Figure 4L). Furthermore, no overt fractures were observed in either Nav1.7Wnt1 or littermate mice demonstrating

(F) Behavioral von Frey responses following SNT surgery on 6-OHDA sympathectomized Nav1.7Advill (red squares, n = 8) and littermate (purple squares, n = 7) mice, in comparison to unsympathectomized littermate controls (white squares, n = 7).

(G) Intraplantar norepinephrine (200 ng) injection sensitizes Nav1.7Wnt1 mice (black line/green square, n = 7) 14 days after SNT surgery, in comparison to vehicle alone in Nav1.7Wnt1 mice 14 days after SNT surgery (green line and squares, n = 6). Data analyzed by two-way analysis of variance followed by the Bonferroni post hoc test. Results are presented as mean ± SEM. **p < 0.01 and ***p < 0.001 (individual points).

See also Figure S2.

A. Oxaliplatin-induced mechanical allodynia

B. Oxaliplatin-induced cold allodynia

C. Nav1.8^DTA mice

D.

E. Cancer-induced bone pain: Limb use

F. Cancer-induced bone pain: Weight bearing

G.

H.

I.

J.

K.

L.

(legend on next page)
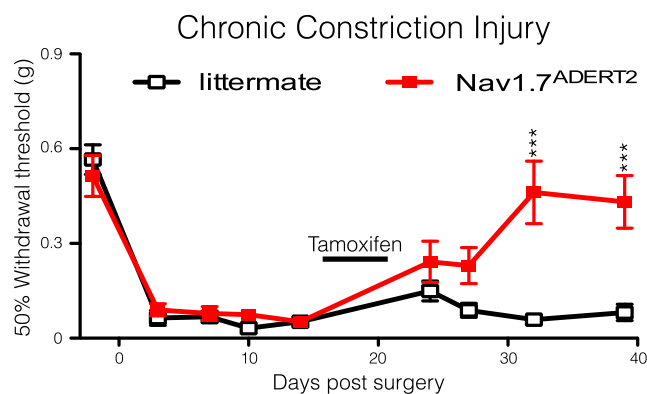
Chronic Constriction Injury

Figure 5. Reversal of CCI-Mediated Mechanical Allodynia after Tamoxifen-Induced Deletion of Nav1.7

Nav1.7^{ADERT2} (red squares, n = 8) mice develop mechanical allodynia normally in comparison to littermate controls (white squares, n = 9) following CCI surgery. However, activation of Advillin-CreERT2 through five daily intraperitoneal tamoxifen injections (2 mg per day) reverses this mechanical allodynia in Nav1.7^{ADERT2} mice but not Advillin-CreERT2 negative littermate controls. Data analyzed by two-way analysis of variance followed by the Bonferroni post hoc test. Results are presented as mean ± SEM. **p < 0.01 and ***p < 0.001 (individual points).

that the observed behavior is related to cancer-induced bone pain and not impaired mobility of the affected leg due to bone fractures.

Deleting Nav1.7 in Adult Mice Reverses Neuropathic Pain

Humans with recessive loss-of-function Nav1.7 mutations are pain free (Cox et al., 2006, Goldberg et al., 2007), but specific high-affinity antagonists of Nav1.7 have so far not produced dramatic analgesic effects (Schmalhofer et al., 2008). It is possible that developmental deficits related to the loss of Nav1.7 in utero could explain some aspects of Nav1.7-dependent pain. To address this, an inducible DRG-specific Nav1.7 knockout mouse strain (Nav1.7^{ADERT2}) was generated using Advillin-CreERT2 (Lau et al., 2011). Lau et al. (2011) show that Advillin-CreERT2 has the same expression pattern as Advillin-Cre, following tamoxifen induction. Figure 5 shows that uninduced Nav1.7^{ADERT2} mice develop mechanical allodynia following CCI surgery in the same manner as littermate controls. However, mechanical allodynia is reversed in Nav1.7^{ADERT2} but not in Advillin-CreERT2-negative, homozygous floxed (Scn9a) Nav1.7 littermate mice following tamoxifen treatment. These data provide further validation of Nav1.7 as a target for analgesic drug development in adult humans.

DISCUSSION

Present views of the organization of the peripheral nervous system have been formed by electrophysiological studies. Gasser showed that fast conducting myelinated A-fibers were involved in pain responses, together with slower conducting C-fibers (Gasser, 1941). There has been a subsequent focus on C-fiber-associated pain largely because the cells are easier to culture and characterize electrophysiologically. The role of specialized sensory neurons that only respond to damaging stimuli in pain pathways was experimentally demonstrated by Burgess and Perl (1967) and Bessou and Perl (1969) and the view that the intensity of a stimulus could change innocuous sensing neurons into damage-sensing neurons (intensity theory) was generally abandoned. Electrophysiological studies suggested that there were a range of different nociceptor subtypes, polymodal nociceptors, cold, mechano-heat (CMH) fibers, and so on, based on the electrical properties of teased fibers (often containing more than one axon) that depolarize in response to various, often superthreshold insults in anesthetized animals. These studies, combined with the now discredited gate-control theory of pain underpinned the view that pain was predominantly a C-fiber-mediated event.

Recent behavioral genetic studies in unanesthetized awake animals are incompatible with this analysis. For example, it is clear that the neurons that respond to noxious thermal (heat) insults are distinct from those involved in noxious mechanosensation when behavioral assays are employed (Abrahamsen et al., 2008; Minett et al., 2012; Mishra et al., 2011). Cell ablation or silencing strategies, where cell markers such as glutamate transporters or sodium channels are used to define and delete/disrupt subsets of sensory neurons, have shown that there is clear specialization in terms of noxious input into the dorsal horn (Abrahamsen et al., 2008; Lagerström et al., 2010, 2011; Minett et al., 2012; Mishra et al., 2011). It is also clear that some A-fibers are nociceptors and some C-fibers are low threshold mechanoreceptors or involved with definition of pleasurable stimuli (Vrontou et al., 2013).

Previously, we reported that neuropathic pain develops normally in mice lacking Nav1.7 and Nav1.8 in the Nav1.8-positive subset of sensory neurons (Nassar et al., 2005). However, the present study provides evidence that some neuropathic pain states depend upon sensory neuron input involving Nav1.7, whereas other neuropathic pain states depend upon the activity of Nav1.7 in both sensory and sympathetic neurons. Thus, Nav1.7 is required for the development of pain in surgical models of neuropathic pain. The sprouting of sympathetic neurons into DRG of damaged nerves depends, surprisingly, upon the

Figure 4. Oxaliplatin-Induced Pain and Cancer-Induced Bone Pain Do Not Require Nav1.7 Expression or Nav1.8⁺ Nociceptors

Nav1.7^{Wnt1} (green squares, n = 7) and littermate (white squares, n = 13) mice treated twice weekly (red arrows) with 3.5 mg/kg oxaliplatin (i.v.) develop both mechanical (A) and cold (B) allodynia. Nav1.8^{DTA} (black squares, n = 10) and littermate mice (white squares, n = 11) treated twice weekly with 3.5 mg/kg oxaliplatin (i.v.) develop both mechanical (C) and cold (D) allodynia. Limb use scores for the affected hind limb (E) and percentage of body weight placed on the affected hind limb (F) of Nav1.7^{Wnt1} (green squares, n = 8) and littermate (white squares, n = 8) mice following cancer induction in the femur. Limb use scores for the affected hind limb (G) and percentage of body weight placed on the affected hind limb (H) of Nav1.8^{DTA} (black squares, n = 9) and, littermate (white squares, n = 8) mice following cancer induction in the femur. Both Nav1.7^{Wnt1} (green column, n = 8) and littermate (white column, n = 8) mice show similar decreases in bone density compared to sham operated mice (black column, n = 5) (I). Example of decreased bone density in a Nav1.7^{Wnt1} (J) and littermate (K) mouse, compared to a sham-operated mouse (L). Scale bars represent 2 mm. Data analyzed by two-way analysis of variance followed by the Bonferroni post hoc test. Results are presented as mean ± SEM. **p < 0.01 and ***p < 0.001 (individual points). See also Figure S3.

presence of Nav1.7 in these cells. The mechanism underlying this phenomenon is unknown, but since the studies of Dogiel and Ramón y Cajal in the 19th century, the existence of sympathetic bundles surrounding sensory neurons in normal animals has been described, with increased sprouting seen following neuronal damage (McLachlan et al., 1993; Ramer and Bisby, 1998b). Sympathetic nerve block has been used effectively in many pain states, and the application of beta blockers has also proved effective in some situations (López-Álvarez et al., 2012). Thus, norepinephrine acting on large diameter sensory neurons seems to be able to lower pain thresholds and cause ongoing pain (Roberts and Foglesong, 1988). Xie et al. showed that repeated stimulation of sympathetic postganglionic neurons within the dorsal ramus enhanced spontaneous activity in large and medium diameter neurons and reduced thresholds of activation in large neurons following SNT surgery (Xie et al., 2010). Interestingly, spontaneously active DRG neurons encapsulated by sympathetic baskets always had conduction velocities above 9 m/s and were clearly distinct from the much slower unmyelinated "classical" nociceptors (Xie et al., 2011). This spontaneous activity could be reduced or eliminated by applying norepinephrine antagonists, or by precutting the gray ramus through which sympathetic fibers innervate the DRG (Xie et al., 2010). We report here that exogenous norepinephrine can cause pain in the absence of Nav1.7, when sensory neurons are damaged (see Figure 2G). A role for EPAC-1-mediated sensitization of Piezo2 mechanotransducing molecules has recently been shown to be important for both touch and allodynia following SNT surgery and is an example of the type of mechanism that may involve peripheral sensitization through nonnociceptive sensory neurons (Eijkelkamp et al., 2013).

Increasing evidence suggests that cancer-induced bone pain is mechanistically different from other chronic pain states, such as neuropathic and inflammatory pain. It has been shown that the neurochemical changes observed in the spinal cord in models of cancer-induced bone pain are different from those observed in inflammatory and neuropathic pain states (Honore et al., 2000). Whereas inflammatory models display increased levels of substance P and calcitonin gene-related peptide in the spinal cord, models of cancer-induced bone pain display no changes in the levels of these neuropeptides (Honore et al., 2000). However, increases in c-Fos expression and dynorphin-expressing neurons have been reported in inflammatory, neuropathic, and cancer-induced bone pain models (Abbadie and Besson, 1992; Schwei et al., 1999; Wagner et al., 1993), suggesting that central pain mechanisms may partially overlap. The behavioral outcomes used to quantify cancer-induced bone pain are substantially different from neuropathic and inflammatory pain models consistent with the existence of distinct underlying mechanisms. Neuropathic and inflammatory pain states have traditionally been measured using threshold responses to evoked stimuli such as von Frey hairs, whereas alternative outcome measures, such as limb use scoring and weight-bearing ratios, have been developed for cancer-induced bone pain models, as measures of evoked pain have been inconsistent and unpredictable (Figures S4A and S4B).

In this study, we demonstrate that cancer-induced bone pain and oxaliplatin-induced pain do not require the peripheral neuronal subpopulations that are essential for acute, inflammatory, and neuropathic pain. Nav1.7 expression within the peripheral nervous system is necessary for acute, inflammatory, and neuropathic pain behavior in mice (Minett et al., 2012; Nassar et al., 2004), as well as in human CIP (Cox et al., 2006, Goldberg et al., 2007) but not for either cancer-induced bone pain or oxaliplatin-induced pain. A role for inflammatory mediators such as tumor necrosis factor-α, nerve growth factor, bradykinins, prostaglandins, and ATP has been identified in the development of cancer-induced bone pain (Falk et al., 2012). Thus, tissue damage and subsequent activation of the immune system associated with the progression of cancer-induced bone pain could sensitize nociceptors to cause ongoing pain. However, the unilateral sensitization of the affected limb demonstrates the importance of peripheral input in ongoing pain. A role for the atypical sodium channel Nax implicated in sodium sensing has recently been described, where lentiviral siRNA knockdown of this channel reverses pain-related behavior associated with tumor growth (Ke et al., 2012). Nax is expressed in the medium to large diameter sensory neurons that are also implicated in oxaliplatin-evoked pain (Ke et al., 2012). Deleting Nav1.7, or ablating the Nav1.8-positive nociceptor population, does not diminish the pain-related behavior associated with either oxaliplatin or cancer-induced bone pain. However, the sodium channel blocker mexiletine is protective against oxaliplatin-induced pain (Egashira et al., 2010). This is consistent with the recent demonstration of an essential role for Nav1.6, in conjunction with delayed rectifier potassium channels in oxaliplatin-evoked pain (Sittl et al., 2012, Deuis et al., 2013). Nav1.6 expression is associated with myelinated A-fibers rather than classical C-fiber-associated nociceptors. Taken together, these observations are consistent with pain resulting from input from neurons that normally subserve innocuous sensation (Table 1).

Further evidence for the complexity of peripheral nociceptive mechanisms comes from sodium channel gene ablation studies. Global deletion of Nav1.3, Nav1.8, or Nav1.9 has quite different effects on cold and mechanical allodynia produced by different neuropathic pain models. These findings provide support for the existence of multiple mechanisms involving different subpopulations of sensory neurons that can produce apparently identical pain phenotypes. Microarray technology has been used to identify dysregulated transcripts common to different pain states (Maratou et al., 2009). The logic of this approach is that a single critical mechanism may underpin the pain caused by a variety of stimuli and provide a potentially useful target of new analgesic drug development. However, the evidence accumulated here suggests that different peripheral cell types and mechanisms lead to phenotypically similar pain states (see Table 2). Müller (1842) first suggested that the quality of a sensation is defined by the central terminations of sensory nerves. Recent advances in the use of genetically encoded calcium indicators should allow us to examine whether redundant mechanisms converge on similar pathways within the spinal cord and midbrain (Zariwala et al., 2012).

These findings have significant implications for clinical practice. Recent attempts to phenotype neuropathic pain patients as a prelude to rational drug treatment are a necessary first step (Backonja et al., 2013), but the present results suggest

Table 1. Peripheral Sodium Channels and Pain Pathways

Pain Modality	Essential Sodium Channel	Peripheral Neuronal Subpopulation
Classical nociceptive pain pathways		
Acute (spinal) heat pain	Nav1.7	Nav1.8-negative sensory neurons
Acute mechanical pain	Nav1.7	Nav1.8-positive sensory neurons
Acute cold pain	Nav1.8	Nav1.8-positive sensory neurons
Inflammatory hyperalgesia	Nav1.7	Nav1.8-positive sensory neurons
Nonnociceptive pain pathways		
Neuropathic mechanical allodynia	Nav1.7	Nav1.8-negative sensory neurons
Neuropathic cold allodynia	Nav1.7	Nav1.8-positive sensory neurons
Sympathetically maintained pain	Nav1.7	Nav1.7-positive sympathetic neurons
Atypical peripheral pain pathways		
Oxaliplatin-evoked allodynia	Nav1.6	A-fiber-associated neurons
Cancer-induced bone pain	Nax	A-fiber-associated neurons

that this useful analysis will require further subdivision into mechanistically distinct pain sets. Given the absence of biomarkers, and the uncertainty about mechanisms involved, the argument for polypharmacy becomes appealing. Triple therapy has proved revolutionary in HIV antiviral therapy (Bernardini and Maggiolo, 2013). There is no reason why multiple therapies should not be routinely used in pain treatment. The often-remarked-upon failure of new analgesic drugs may be linked to a failure to distinguish mechanistically distinct pain syndromes, and an inability to tease out useful effects of drugs on subsets of pain patients in the overall noise of nonresponders.

In summary, we have provided evidence that some pain states do not involve classical nociceptor activation, consistent with the proposal of the intensity theory that suggests neurons responding to innocuous stimuli may activate central pain pathways in some circumstances. The overwhelming evidence for redundancy in pain mechanisms coupled with a simplistic classification of nociceptive mechanisms on the basis of early electrophysiological studies helps to explain recent problems in developing analgesic drugs. Further mechanistic studies and a combined therapeutic attack on critical pain mediators such as norepinephrine and proinflammatory cytokines as well as the electrical apparatus that underpins peripheral signaling to the CNS is a logical route to pain treatment in the future.

EXPERIMENTAL PROCEDURES

Genotyping

Genomic DNA was isolated from ear notches as described previously (Akopian et al., 1999; Nassar et al., 2006; Abrahamsen et al., 2008; Minett et al., 2012; Ostman et al., 2008).

Behavioral Testing

Animal experiments were approved by the UK Home Office and UCL ethics committee. Touch perception thresholds were measured using the up-down method for obtaining the 50% threshold using von Frey hairs (Chaplan et al., 1994). Behavioral response to cooling (approximately 10°C –15°C) by acetone test was performed (Bautista et al., 2006).

Spinal Nerve Transection at the Fifth Lumbar Segment

A modified version of the Kim and Chung model (Kim and Chung, 1992) of peripheral neuropathy was adapted for use on mice (Minett et al., 2012). Acetone and von Frey thresholds were recorded at baseline and up to 28 days after surgery.

Chronic Constriction Injury of the Sciatic Nerve

The Bennett and Xie model of peripheral neuropathy (Bennett and Xie, 1988) was adapted for use on mice. Acetone and von Frey thresholds were recorded at baseline and up to 28 days after surgery.

Oxaliplatin-Induced Pain

Oxaliplatin (Sigma) was administered intravenously by tail vein injection (3.5 mg/kg). Mice received a total of four injections separated by 3 then 4 days (Renn et al., 2011).

Cancer-Induced Bone Pain

A model of metastatic bone pain was introduced by intrafemoral injection of LL/2 lung carcinoma cells (Clohisy et al., 1996). Spontaneous and movement-evoked pain response measures were used to evaluate pain behavior up to 16 days after induction (Falk et al., 2013).

Induction of Advillin-CreERT2

Advillin-CreERT2 expression was induced via a series of five consecutive daily 2 mg intraperitoneal (i.p.) injections of tamoxifen (Sigma-Aldrich) (Lau et al., 2011).

Chemical Sympathectomy

6-OHDA (Sigma) was dissolved in sterile saline containing 0.01% (w/v) ascorbic acid (vehicle) and was injected intraperitoneally at a concentration of 200 mg/kg (Leo et al., 1998). Control mice received an equivalent volume of vehicle alone.

Immunocytochemistry

DRGs were excised from animals perfused with 4% paraformaldehyde. Serial 10 μm sections were collected. Slides were washed and blocked in 10% goat serum in PBS +0.3% Triton for 1 hr at room temperature and incubated in the primary antibody overnight at 4°C. Primary antibodies were detected by incubating with the secondary antibody at room temperature for 2 hr.

Quantification of Sympathetic Sprouting

Tissue samples were visualized and captured in monochrome and pseudocolored using HCImage 2.0.1.16. ImageJ64 analysis software (NIH) was used to quantify sympathetic axons. To generate innervation density data, the total area of DRG cell layer, excluding axonal tracts, was measured. Following this, the length of TH-positive axons within the marked area was measured. A reference image with known grid size was used to calculate units.

Quantification of Bone Degradation

Following dissection and fixation, radiographic images of the distal femur head were obtained using a digital camera inside an enclosed cabinet during exposure to an X-ray source (Faxitron MX-20). Each X-ray image was calibrated to a standard aluminum wedge and the grayscale intensity quantified using ImageJ. The calibrated grayscale value was used to quantify the relative bone density of the distal femur for statistical analysis.

Statistics

Data were analyzed using the GraphPad Prism 5. Student's t test (two-tailed) was used for comparison of difference between two distributions. Multiple groups were compared using one-way or two-way analysis of variance with the Bonferroni post hoc test.

Table 2. Summary of Distinct Neuronal Subpopulations and Mechanisms Underlying Different Neuropathic Pain Models

VGSC	Deleted from	Chronic Constriction Injury		Spinal Nerve Transection		Oxaliplatin-Induced Pain	
		Cold Allodynia	Mechanical Allodynia	Cold Allodynia	Mechanical Allodynia	Cold Allodynia	Mechanical Allodynia
Nav1.3	CNS/PNS	attenuated	attenuated	normal	normal	normal	normal
Nav1.7	Nociceptors	lost	normal	normal	normal	normal	normal
	Sensory neurons	lost	lost	normal	normal	normal	normal
	Sympathetic and sensory neurons	lost	lost	lost	lost	normal	normal
Nav1.8	Nociceptors	attenuated	normal	normal	normal	normal	normal
Nav1.9	Nociceptors	attenuated	normal	normal	normal	normal	normal

VGSC, voltage-gated sodium channel; PNS, peripheral nervous system; CNS, central nervous system.

SUPPLEMENTAL INFORMATION

AUTHOR CONTRIBUTIONS

ACKNOWLEDGMENTS

REFERENCES

Abbadie, C., and Besson, J.M. (1992). c-fos expression in rat lumbar spinal cord during the development of adjuvant-induced arthritis. Neuroscience 48, 985–993.

Abrahamsen, B., Zhao, J., Asante, C.O., Cendan, C.M., Marsh, S., Martinez-Barbera, J.P., Nassar, M.A., Dickenson, A.H., and Wood, J.N. (2008). The cell and molecular basis of mechanical, cold, and inflammatory pain. Science 321, 702–705.

Aguirre, J., Del Moral, A., Cobo, I., Borgeat, A., and Blumenthal, S. (2012). The role of continuous peripheral nerve blocks. Anesthesiol. Res. Pract. 2012, 560879.

Akopian, A.N., Souslova, V., England, S., Okuse, K., Ogata, N., Ure, J., Smith, A., Kerr, B.J., McMahon, S.B., Boyce, S., et al. (1999). The tetrodotoxin-resistant sodium channel SNS has a specialized function in pain pathways. Nat. Neurosci. 2, 541–548.

Backonja, M.M., Attal, N., Baron, R., Bouhassira, D., Drangholt, M., Dyck, P.J., Edwards, R.R., Freeman, R., Gracely, R., Haanpaa, M.H., et al. (2013). Value of quantitative sensory testing in neurological and pain disorders: NeuPSIG consensus. Pain 154, 1807–1819.

Baron, R., Levine, J.D., and Fields, H.L. (1999). Causalgia and reflex sympathetic dystrophy: does the sympathetic nervous system contribute to the generation of pain? Muscle Nerve 22, 678–695.

Bautista, D.M., Jordt, S.-E., Nikai, T., Tsuruda, P.R., Read, A.J., Poblete, J., Yamoah, E.N., Basbaum, A.I., and Julius, D. (2006). TRPA1 mediates the inflammatory actions of environmental irritants and proalgesic agents. Cell 124, 1269–1282.

Bennett, G.J., and Xie, Y.K. (1988). A peripheral mononeuropathy in rat that produces disorders of pain sensation like those seen in man. Pain 33, 87–107.

Bernardini, C., and Maggiolo, F. (2013). Triple-combination rilpivirine, emtricitabine, and tenofovir (Complera™/Eviplera™) in the treatment of HIV infection. Patient Prefer Adherence 7, 531–542.

Bessou, P., and Perl, E.R. (1969). Response of cutaneous sensory units with unmyelinated fibers to noxious stimuli. J. Neurophysiol. 32, 1025–1043.

Brumovsky, P., Villar, M.J., and Hökfelt, T. (2006). Tyrosine hydroxylase is expressed in a subpopulation of small dorsal root ganglion neurons in the adult mouse. Exp. Neurol. 200, 153–165.

Burgess, P.R., and Perl, E.R. (1967). Myelinated afferent fibres responding specifically to noxious stimulation of the skin. J. Physiol. 190, 541–562.

Campbell, J.N., and Meyer, R.A. (2006). Mechanisms of neuropathic pain. Neuron 52, 77–92.

Chaplan, S.R., Bach, F.W., Pogrel, J.W., Chung, J.M., and Yaksh, T.L. (1994). Quantitative assessment of tactile allodynia in the rat paw. J. Neurosci. Methods 53, 55–63.

Clohisy, D.R., Palkert, D., Ramnaraine, M.L., Pekurovsky, I., and Oursler, M.J. (1996). Human breast cancer induces osteoclast activation and increases the number of osteoclasts at sites of tumor osteolysis. J. Orthop. Res. 14, 396–402.

Cox, J.J., Reimann, F., Nicholas, A.K., Thornton, G., Roberts, E., Springell, K., Karbani, G., Jafri, H., Mannan, J., Raashid, Y., et al. (2006). An SCN9A channelopathy causes congenital inability to experience pain. Nature 444, 894–898.

Danielian, P.S., Muccino, D., Rowitch, D.H., Michael, S.K., and McMahon, A.P. (1998). Modification of gene activity in mouse embryos in utero by a tamoxifen-inducible form of Cre recombinase. Curr. Biol. 8, 1323–1326.

Descoeur, J., Pereira, V., Pizzoccaro, A., Francois, A., Ling, B., Maffre, V., Couette, B., Busserolles, J., Courteix, C., Noel, J., et al. (2011). Oxaliplatin-induced cold hypersensitivity is due to remodelling of ion channel expression in nociceptors. EMBO Mol Med 3, 266–278.

Deuis, J.R., Zimmermann, K., Romanovsky, A.A., Possani, L.D., Cabot, P.J., Lewis, R.J., and Vetter, I. (2013). An animal model of oxaliplatin-induced cold allodynia reveals a crucial role for Nav1.6 in peripheral pain pathways. Pain 154, 1749–1757.

Egashira, N., Hirakawa, S., Kawashiri, T., Yano, T., Ikesue, H., and Oishi, R. (2010). Mexiletine reverses oxaliplatin-induced neuropathic pain in rats. J. Pharmacol. Sci. 112, 473–476.

Eijkelkamp, N., Linley, J.E., Baker, M.D., Minett, M.S., Cregg, R., Werdehausen, R., Rugiero, F., and Wood, J.N. (2012). Neurological perspectives on voltage-gated sodium channels. Brain 135, 2585–2612.

Eijkelkamp, N., Linley, J.E., Torres, J.M., Bee, L., Dickenson, A.H., Gringhuis, M., Minett, M.S., Hong, G.S., Lee, E., Oh, U., et al. (2013). A role for Piezo2 in EPAC1-dependent mechanical allodynia. Nat Commun 4, 1682.

Falk, S., Uldall, M., and Heegaard, A.-M. (2012). The role of purinergic receptors in cancer-induced bone pain. J. Osteoporos. 2012, 758181.

Falk, S., Uldall, M., Appel, C., Ding, M., and Heegaard, A.-M. (2013). Influence of sex differences on the progression of cancer-induced bone pain. Anticancer Res. 33, 1963–1969.

García-Poblete, E., Fernández-García, H., Moro-Rodríguez, E., Catalá-Rodríguez, M., Rico-Morales, M.L., García-Gómez-de-las-Heras, S., and Palomar-Gallego, M.A. (2003). Sympathetic sprouting in dorsal root ganglia (DRG): a recent histological finding? Histol. Histopathol. 18, 575–586.

Gasser, H.S. (1941). The classification of nerve fibers. Ohio J. Sci. 41, 145–159.

Goldberg, Y.P., MacFarlane, J., MacDonald, M.L., Thompson, J., Dube, M.P., Mattice, M., Fraser, R., Young, C., Hossain, S., Pape, T., et al. (2007). Loss-of-function mutations in the Nav1.7 gene underlie congenital indifference to pain in multiple human populations. Clin. Genet. 71, 311–319.

Honore, P., Rogers, S.D., Schwei, M.J., Salak-Johnson, J.L., Luger, N.M., Sabino, M.C., Clohisy, D.R., and Mantyh, P.W. (2000). Murine models of inflammatory, neuropathic and cancer pain each generates a unique set of neurochemical changes in the spinal cord and sensory neurons. Neuroscience 98, 585–598.

Ke, C.B., He, W.S., Li, C.J., Shi, D., Gao, F., and Tian, Y.K. (2012). Enhanced SCN7A/Nax expression contributes to bone cancer pain by increasing excitability of neurons in dorsal root ganglion. Neuroscience 227, 80–89.

Kim, S.H., and Chung, J.M. (1992). An experimental model for peripheral neuropathy produced by segmental spinal nerve ligation in the rat. Pain 50, 355–363.

Kim, K.J., Yoon, Y.W., and Chung, J.M. (1997). Comparison of three rodent neuropathic pain models. Exp. Brain Res. 113, 200–206.

Kinnane, N. (2007). Burden of bone disease. Eur. J. Oncol. Nurs. 11 (Suppl 2), S28–S31.

Lagerström, M.C., Rogoz, K., Abrahamsen, B., Persson, E., Reinius, B., Nordenankar, K., Olund, C., Smith, C., Mendez, J.A., Chen, Z.-F., et al. (2010). VGLUT2-dependent sensory neurons in the TRPV1 population regulate pain and itch. Neuron 68, 529–542.

Lagerström, M.C., Rogoz, K., Abrahamsen, B., Lind, A.-L., Olund, C., Smith, C., Mendez, J.A., Wallén-Mackenzie, Å., Wood, J.N., and Kullander, K. (2011). A sensory subpopulation depends on vesicular glutamate transporter 2 for mechanical pain, and together with substance P, inflammatory pain. Proc. Natl. Acad. Sci. USA 108, 5789–5794.

Lallemend, F., and Ernfors, P. (2012). Molecular interactions underlying the specification of sensory neurons. Trends Neurosci. 35, 373–381.

Lau, J., Minett, M.S., Zhao, J., Dennehy, U., Wang, F., Wood, J.N., and Bogdanov, Y.D. (2011). Temporal control of gene deletion in sensory ganglia using a tamoxifen-inducible Advillin-Cre-ERT2 recombinase mouse. Mol. Pain 7, 100.

Leo, N.A., Callahan, T.A., and Bonneau, R.H. (1998). Peripheral sympathetic denervation alters both the primary and memory cellular immune responses to herpes simplex virus infection. Neuroimmunomodulation 5, 22–35.

Liu, X., Chung, K., and Chung, J.M. (1999). Ectopic discharges and adrenergic sensitivity of sensory neurons after spinal nerve injury. Brain Res. 849, 244–247.

López-Álvarez, S., Mayo-Moldes, M., Zaballos, M., Iglesias, B.G., and Blanco-Dávila, R. (2012). Esmolol versus ketamine-remifentanil combination for early postoperative analgesia after laparoscopic cholecystectomy: a randomized controlled trial. Can. J. Anaesth. 59, 442–448.

Maratou, K., Wallace, V.C.J., Hasnie, F.S., Okuse, K., Hosseini, R., Jina, N., Blackbeard, J., Pheby, T., Orengo, C., Dickenson, A.H., et al. (2009).

Comparison of dorsal root ganglion gene expression in rat models of traumatic and HIV-associated neuropathic pain. Eur. J. Pain 13, 387–398.

McLachlan, E.M., Jänig, W., Devor, M., and Michaelis, M. (1993). Peripheral nerve injury triggers noradrenergic sprouting within dorsal root ganglia. Nature 363, 543–546.

Mercadante, S. (1997). Malignant bone pain: pathophysiology and treatment. Pain 69, 1–18.

Minett, M.S., Nassar, M.A., Clark, A.K., Passmore, G., Dickenson, A.H., Wang, F., Malcangio, M., and Wood, J.N. (2012). Distinct Nav1.7-dependent pain sensations require different sets of sensory and sympathetic neurons. Nat Commun 3, 791–799.

Mishra, S.K., Tisel, S.M., Orestes, P., Bhangoo, S.K., and Hoon, M.A. (2011). TRPV1-lineage neurons are required for thermal sensation. EMBO J. 30, 582–593.

Müller, J. (1842). Elements of Physiology (London: Taylor and Walton).

Nassar, M.A., Stirling, L.C., Forlani, G., Baker, M.D., Matthews, E.A., Dickenson, A.H., and Wood, J.N. (2004). Nociceptor-specific gene deletion reveals a major role for Nav1.7 (PN1) in acute and inflammatory pain. Proc. Natl. Acad. Sci. USA 101, 12706–12711.

Nassar, M.A., Levato, A., Stirling, L.C., and Wood, J.N. (2005). Neuropathic pain develops normally in mice lacking both Na(v)1.7 and Na(v)1.8. Mol. Pain 1, 24.

Nassar, M.A., Baker, M.D., Levato, A., Ingram, R., Mallucci, G., McMahon, S.B., and Wood, J.N. (2006). Nerve injury induces robust allodynia and ectopic discharges in Nav1.3 null mutant mice. Mol. Pain 2, 33.

Ostman, J.A., Nassar, M.A., Wood, J.N., and Baker, M.D. (2008). GTP up-regulated persistent Na+ current and enhanced nociceptor excitability require NaV1.9. J. Physiol. 586, 1077–1087.

Ramer, M.S., and Bisby, M.A. (1998a). Sympathetic axons surround neuropeptide-negative axotomized sensory neurons. Neuroreport 9, 3109–3113.

Ramer, M.S., and Bisby, M.A. (1998b). Normal and injury-induced sympathetic innervation of rat dorsal root ganglia increases with age. J. Comp. Neurol. 394, 38–47.

Ramer, M.S., and Bisby, M.A. (1998c). Differences in sympathetic innervation of mouse DRG following proximal or distal nerve lesions. Exp. Neurol. 152, 197–207.

Renn, C.L., Carozzi, V.A., Rhee, P., Gallop, D., Dorsey, S.G., and Cavaletti, G. (2011). Multimodal assessment of painful peripheral neuropathy induced by chronic oxaliplatin-based chemotherapy in mice. Mol. Pain 7, 29.

Roberts, W.J. (1986). A hypothesis on the physiological basis for causalgia and related pains. Pain 24, 297–311.

Roberts, W.J., and Foglesong, M.E. (1988). Spinal recordings suggest that wide-dynamic-range neurons mediate sympathetically maintained pain. Pain 34, 289–304.

Schmalhofer, W.A., Calhoun, J., Burrows, R., Bailey, T., Kohler, M.G., Weinglass, A.B., Kaczorowski, G.J., Garcia, M.L., Koltzenburg, M., and Priest, B.T. (2008). ProTx-II, a selective inhibitor of NaV1.7 sodium channels, blocks action potential propagation in nociceptors. Mol. Pharmacol. 74, 1476–1484.

Schwei, M.J., Honore, P., Rogers, S.D., Salak-Johnson, J.L., Finke, M.P., Ramnaraine, M.L., Clohisy, D.R., and Mantyh, P.W. (1999). Neurochemical and cellular reorganization of the spinal cord in a murine model of bone cancer pain. J. Neurosci. 19, 10886–10897.

Seltzer, Z., Dubner, R., and Shir, Y. (1990). A novel behavioral model of neuropathic pain disorders produced in rats by partial sciatic nerve injury. Pain 43, 205–218.

Shields, S.D., Ahn, H.-S., Yang, Y., Han, C., Seal, R.P., Wood, J.N., Waxman, S.G., and Dib-Hajj, S.D. (2012). Nav1.8 expression is not restricted to nociceptors in mouse peripheral nervous system. Pain 153, 2017–2030.

Sittl, R., Lampert, A., Huth, T., Schuy, E.T., Link, A.S., Fleckenstein, J., Alzheimer, C., Grafe, P., and Carr, R.W. (2012). Anticancer drug oxaliplatin induces acute cooling-aggravated neuropathy via sodium channel subtype

Na(V)1.6-resurgent and persistent current. Proc. Natl. Acad. Sci. USA *109*, 6704–6709.

Torebjörk, E., Wahren, L., Wallin, G., Hallin, R., and Koltzenburg, M. (1995). Noradrenaline-evoked pain in neuralgia. Pain *63*, 11–20.

Velasco, R., and Bruna, J. (2010). [Chemotherapy-induced peripheral neuropathy: an unresolved issue]. Neurologia *25*, 116–131.

Vrontou, S., Wong, A.M., Rau, K.K., Koerber, H.R., and Anderson, D.J. (2013). Genetic identification of C fibres that detect massage-like stroking of hairy skin in vivo. Nature *493*, 669–673.

Wagner, R., DeLeo, J.A., Coombs, D.W., Willenbring, S., and Fromm, C. (1993). Spinal dynorphin immunoreactivity increases bilaterally in a neuropathic pain model. Brain Res. *629*, 323–326.

Waxman, S.G. (2013). Painful Na-channelopathies: an expanding universe. Trends Mol. Med. *19*, 406–409.

Xie, W., Strong, J.A., and Zhang, J.-M. (2010). Increased excitability and spontaneous activity of rat sensory neurons following in vitro stimulation of sympathetic fiber sprouts in the isolated dorsal root ganglion. Pain *151*, 447–459.

Xie, W., Strong, J.A., Mao, J., and Zhang, J.-M. (2011). Highly localized interactions between sensory neurons and sprouting sympathetic fibers observed in a transgenic tyrosine hydroxylase reporter mouse. Mol. Pain *7*, 53.

Zariwala, H.A., Borghuis, B.G., Hoogland, T.M., Madisen, L., Tian, L., De Zeeuw, C.I., Zeng, H., Looger, L.L., Svoboda, K., and Chen, T.W. (2012). A Cre-dependent GCaMP3 reporter mouse for neuronal imaging in vivo. J. Neurosci. *32*, 3131–3141.